Journal of Advanced Research 24 (2020) 159–166

Contents lists available at ScienceDirect

Journal of Advanced Research

journal homepage: www.elsevier.com/locate/jare

Double layer MOFs M-ZIF-8@ZIF-67: The adsorption capacity and removal mechanism of fipronil and its metabolites from environmental water and cucumber samples

Tengfei Li [a,b,1], Meng Lu [a,b,1], Yuhang Gao [a], Xiaodong Huang [a], Guangyang Liu [a,*], Donghui Xu [a,*]

[a] Institute of Vegetables and Flowers, Chinese Academy of Agricultural Sciences, Key Laboratory of Vegetables Quality and Safety Control, Ministry of Agriculture and Rural Affairs of China, Beijing 100081, China
[b] College of Life Sciences and Engineering, Hebei University of Engineering, Handan 056000, China

HIGHLIGHTS

- Magnetic double-layer MOFs was prepared with porous crystal structure.
- MMOFs have high adsorption capacity for fipronil pesticides.
- Adsorption model analysis fitted the Freundlich adsorption model.
- Removal rate of fipronil in water and cucumber were 70.9–99.7%.

GRAPHICAL ABSTRACT

ARTICLE INFO

Article history:
Received 5 August 2019
Revised 25 March 2020
Accepted 31 March 2020
Available online 5 April 2020

Keywords:
Double layer Metal-organic framework
M-ZIF-8@ZIF-67
Adsorption
Removal
Water and Cucumber samples

ABSTRACT

In this study, a novel metal-organic framework (M-ZIF-8@ZIF-67) was successfully prepared using the single layer Fe_3O_4-ZIF-8 as magnetic core and wrapped a layer of ZIF-67 outer. This M-ZIF-8@ZIF-67 was employed as an adsorbent for the adsorption and removal of fipronil and its metabolites from environmental water and cucumber samples. The characterization results suggested that M-ZIF-8@ZIF-67 has the double layer structure a polyhedral structure with uniform pores, while ZIF-67 was successfully coated on the surface of Fe_3O_4-ZIF-8. The unique structure endowed M-ZIF-8@ZIF-67 a high surface area (219 m^2/g) and high adsorption capacity for fipronil, fipronil desulfinyl, fipronil sulfide and fipronil sulfone. To our knowledge, this is the first report detailing the adsorption properties of M-ZIF-8@ZIF-67 with double layer structure relating to the adsorption and removal of pesticides. Furthermore, the adsorption model analysis demonstrated that the static adsorption data fitted the Freundlich bimolecular layer adsorption model better than the Langmuir monolayer adsorption model. This study indicates that M-ZIF-8@ZIF-67 has significant potential in the adsorption and removal of fipronil and its metabolites in water and vegetable samples.

Introduction

In recent years, pesticides have been used excessively to improve the output of agricultural products [1]. Fipronil is a phenyl pyrazole insecticide exhibiting high insecticidal activity [2] that is

Peer review under responsibility of Cairo University.
* Corresponding authors.
E-mail addresses: liuguangyang@caas.cn (G. Liu), xudonghui@caas.cn (D. Xu).
[1] Co-authors with equal contributions.

https://doi.org/10.1016/j.jare.2020.03.013
2090-1232/

widely used to protect agricultural products. Fipronil and its metabolites, including fipronil desulfinyl, fipronil sulfide and fipronil sulfone [3]. However, Fipronil and its metabolites exhibit strong toxicity and therefore pose a threat to human health and the environment [4,5]. Effective adsorption and removal of residual pesticides from vegetables and environmental waters is an important scientific area.

There are numerous methods have been employed to remove pesticides from aqueous environments, such as adsorption, membrane separation, biodegradation and photocatalytic degradation [6]. Among these methods, adsorption technique based on solid adsorbents can efficiency for convenient and quick adsorption and removal of organic pollutants in water and food samples [7]. Widely-known adsorbents materials for the removal of pesticides are metal oxides, silica particles, carbon materials, magnetic materials and porous polymers [8]. Because of low adsorption capacities and tedious operation procedures, challenges remain to develop novel adsorbent materials that can be used efficiently to adsorb and remove a variety of pesticides. Metal-organic frameworks (MOFs) are considered as effective adsorbents because of the interactions between the adsorbents and the target object include electrostatic interactions, hydrogen bond interactions and π-π conjugate forces [9–12]. MOFs demonstrate some advantages which are shown as follows: First, MOFs possess uniform and regular pore structures, larger pore dimensions and specific surface areas. The adsorption processes of different organic pollutants occur mainly on the surface or inside of MOFs [13]. In additional, the structure of synthesized MOFs can be tailored and introduced characteristic performance by varying the functional groups, organic ligands and metal ions [14]. More importantly, the external unsaturated active sites of MOFs will facilitate improving its adsorption property and removal capacity for pesticides residues [15].

According to the previous literatures, zeolitic imidazolate frameworks (ZIFs) can be synthesized *via* a simple and convenient method and present potential application in pesticide adsorption [16–18]. ZIF-8 and ZIF-67 has three-dimensional topology similar to zeolites, and attracts much interest to develop potential absorbent for pesticides adsorption [19]. However, the main drawbacks such as low specific surface areas, poor structural stability and difficult separation limit its further applications [20]. Preparing the double-layer structure of hybrid MOFs by coating ZIF-67 onto the surface of ZIF-8 may be a feasible way to overcome the abovementioned shortcomings. Owing to the same ligand (2-methylimidazole), combining ZIF-8 and ZIF-67 together by using epitaxial growth method to improve the performance of absorbents is believed to be a considered potential strategy [21–23]. The bilayer structure of ZIF-8@ZIF-67 composite material could exhibit numerous similar pore structures, which will enhance the adsorption and removal capacities for pesticides residues [24].

In this paper, we have designed a novel magnetic bilayer MOFs material (M-ZIF-8@ZIF-67) by using one-pot synthetic method and layer-by-layer self-assembly. For the first time, M-ZIF-8@ZIF-67 was used as an adsorbent to adsorb and remove fipronil and its metabolites in water and vegetable samples. M-ZIF-8@ZIF-67 was then characterized and their adsorption mechanism were verified by static adsorption, adsorption kinetics and adsorption model analysis. After that, the key factor and SPE procedure may affect the adsorption capacity and rate were then optimized. Furthermore, the adsorption properties of M-ZIF-8@ZIF-67 for fipronil and its metabolites in cucumber and ambient water were studied in details. This could lay a research foundation for functionalizing double-layer MOFs into the micro-extraction fiber needle, and constructing rapid enrichment method and novel SPE equipment.

Experimental

Chemicals and materials

Fipronil, fipronil desulfiny, fipronil sulfone and fipronil sulfide were obtained from Sigma-Aldrich (St. Louis, Mo. USA). 2-methylimidazole was purchased from Aladdin Industrial Corporation (Shanghai, China). $FeSO_4{\cdot}7H_2O$, $FeCl_3{\cdot}6H_2O$, $Zn(NO_3)_2{\cdot}6H_2O$ and $Co(NO_3)_2$ were purchased from Sinopharm Chemical Reagent Co. Ltd. All other materials were of analytical reagent grade and purchased from the Beijing Chemical Reagent factory (Beijing, China).

Apparatus

The particle size and surface morphologies of MOFs were investigated using scanning electron microscopy (SEM, JSM-6300, JEOL, Japan). FT-IR spectra were recorded using an FI-IR-8400 spectrometer (Shimad Zu, Japan). X-ray powder diffraction (XRD) was obtained using a D8 Advance x-ray powder diffractometer (Bruker, Germany). To investigate the magnetic properties of all products, vibrating sample magnetometry (VSM, Lake Shore 7410 USA) was performed. High-performance liquid chromatography-tandem mass spectrometry (HPLC-MS/MS, LC-30A, MS8050, Shimadzu, Japan) was used to verify the adsorption capacity of the materials.

Preparation of Fe_3O_4

Fe_3O_4 nanoparticles were synthesized according to a previously reported chemical synthesis method [25]. Generally, $Fe_2SO_4{\cdot}7H_2O$ (0.7 g) and $FeCl_3{\cdot}6H_2O$ powders (1.2 g) were dissolved in ultrapure water (20 mL, filtration membrane 0.22 μm), and thereafter, were mixed with 240 mL ultrapure water under N_2 protection in a three-necked flask. The solution was vigorously stirred using a mechanical stirrer at 80 °C for 30 min. An ammonium hydroxide (10 mL) solution was then added to the mixture prior to vigorously stirring for an additional 30 min at 80 °C. The mixture solution was then cooled to room temperature. Finally, the material was washed twice with ethanol and water.

Preparation of M-ZIF-8/ZIF-67

M-ZIF-8/ZIF-67 was prepared using a reported method with slight modification [16]. $Zn(NO_3)_2{\cdot}6H_2O$ was dispersed in water (5 mL) and added to an aqueous solution of Fe_3O_4 (20 mL) under vigorous stirring for 30 min., An aqueous solution (20 mL) containing 2-methylimidazole (0.82 g) was added into this mixture and then stirred for 1 hr. After that, a solution comprising $Co(NO_3)_2$ (0.34 g) dispersed in water (5 mL) was mixed for 30 min. Finanlly, the aqueous solution containing 2-methylimidazole was added into the abovementioned mixture and reacted under magnetic stirring for l h. The mixed solution was separated using a magnet, washed twice with ethanol and water to remove unreacted chemicals, and thereafter, dried in a vacuum oven at 60 °C.

Adsorption experiments

The synthesized M-ZIF-8@ZIF-67 materials were completely dried prior to being mixed with pesticide aqueous solutions. 100 mg/L stock pesticide-containing acetone solutions were prepared and then pesticides mixture with concentration of 100 mg/L was diluted with ultrapure water into different working solutions. To obtain the desired adsorption performance for the M-MOF materials [26], the solutions were added at low molar

mass HCL levels to adjust the pH of the solutions to 6, with a target M-ZIF-8@ZIF-67 loading of 15 mg being dispersed into the working solutions (4 mL) containing the four different concentrations of pesticides (0–20 mg/L). Thereafter, the mixtures were oscillated for 45 min at room temperature. M-ZIF-8@ZIF-67 was separated using a magnet and extracted from the pesticide supernatants of varying concentrations (or the supernatant was diluted by methanol) and analyzed by HPLC-MS/MS.

The static adsorption binding capacity of the M-MOF materials in fipronil and its derivative pesticides were calculated using (Eq. (1)):

$$Q_e = (C_o - C_e)V/M \quad (1)$$

where Q_e is the static binding capacity (m/mg), C_o is the initial pesticide concentration of the solution (mg/L), C_e is the end pesticide concentration of the solution (mg/L), V is the volume of the initial pesticide solution, and *M* is the quantity of the material (mg).

The adsorption isotherm was estimated based on the following formulae:

$$1/Q_{eq} = 1/KC_{eq}Q_{max} + 1/Q_{max} \quad (2)$$

$$\ln Q_{eq} = \ln K_f + (1/n)\ln C_{eq} \quad (3)$$

The Langmuir (Eq. (2)) and Freundlich (Eq. (3)) models were used, where *K* is the adsorption constant derived from the Langmuir model (L/mg), $Q_{max}Q_{max}$ is the saturated adsorption capacity (mg/g), K_f is the adsorption constant derived from the Freundlich model (mg/g), and *1/n* is the adsorption strength, or degree, of surface inhomogeneity.

The adsorption kinetics was verified using a pseudo-second-order kinetic model (Eq. (4)) [27]:

$$\frac{t}{Q_t} = \frac{1}{k_2}Q_{2cal}^2 + \frac{t}{Q_{2cal}} \quad (4)$$

where Q_t (mg/g) is the static binding capacity at a specific oscillation time (min), Q_{2cal}^2 (mg/g) is the theoretical adsorption capacity at adsorption saturation, and k_2 is the adsorption rate constant (g/(mg·min)) for pseudo-second-order kinetics. The adsorption kinetics of the experimental process is as follows: M-MOF materials (15 mg) were mixed with aqueous solutions containing the four pesticides (4 mL, 5 mg/L) and thereafter, oscillated for different periods of time.

Sample preparation

Underground water, river water, and tap water were collected from Beijing, Tianjin and Lang Fang City, Hebei Province, respectively. Cucumbers are purchased at local supermarkets, vegetable markets and vegetable production base in Lang fang, Hebei Province, respectively. The purchased vegetables had no target pesticides residues after testing using HPLC-MS/MS, and the target pesticides were then added to simulate the positive samples of pesticide contamination. The practicability and anti-matrix interference ability of the method were investigated. All of the water samples were filtered through a microporous injection filter membrane prior to adding to the pesticide working solutions, to give a final water sample concentration of (5, 10, 15, 20, 50, 100, 200 and 400 μg/L) The cucumbers were ground to a pulp, centrifuged and filtered through the membrane. The cucumber supernatant was collected and spiked with varying pesticide concentrations. Synthesis process of a double-layer metal–organic framework (MOF) is show in Fig. 1.

Results and discussion

Characterization of M-ZIF-8@ZIF-67

SEM analysis was used to study the morphology and particle size of the prepared M-ZIF-8 and M-ZIF-8@ZIF-67 materials. Fig. 2a shows the emergence of the polyhedral structure of the Fe_3O_4-ZIF-8 framework with nanometer apertures of a narrow size distribution. Fig. 2b shows ZIF-67 surface coverage over the M-ZIF-8 surface. ZIF-67 exhibits a porous structure having a narrow size distribution similar to the M-ZIF-8 structure, likely as a result of similar cell parameters.

XRD analysis of the MOF materials also verified similar cell parameters [28]. Fig. 3a shows that M-ZIF-8@ZIF-67 obtains a highly porous block structure. The microporous structure of the polyhedron significantly improves the adsorption of pesticides by M-ZIF-8@ZIF-67. The composition and distribution of atoms on the surface of the materials were characterized by energy-dispersive X-ray spectroscopy analysis (Fig. 3b). The iron concentration located at the M-MOF surface was lower than on the corresponding M-ZIF-8, however, the Co concentration located at the M-MOF surface was higher than that on the M-ZIF-8 surface. The results show that M-ZIF-8 was completely covered by ZIF-67 and the elemental composition of M-ZIF-8 was unchanged.

Based on the study of the magnetic properties of M-MOF, the hysteresis loop obtained by VSM was used to evaluate the magnetic properties of M-MOF [29]. Fig. 3c shows that remanence and the coercivity values of all materials were 0. This indicates that all materials have super-magnetic properties, therefore, magnetic separation can be performed using an external magnetic field. The saturation magnetization values of Fe_3O_4, Fe_3O_4-ZIF-8, and magnetic MOF were 85.56, 59.76, 51.93. Although the magnetic properties decrease in turn, the final product still exhibits sufficient magnetic properties so as not to affect the separation process. The VSM data indicate that the magnetic particles have been successfully synthesized within the interior of the material.

Fig. 4a shows the FT-IR spectrum of the synthesized materials. The characteristic absorption peaks of the synthetic materials (Fe_3O_4-ZIF-8@ ZIF-67) have been previously reported. The magnetic materials exhibit a peak at 560.24 cm^{-1}, attributed to the vibration of Fe—O—Fe, which indicates that the magnetic nanoparticles were successfully coated onto the core material. The magnetic properties of M-ZIF-8 and M-ZIF-8@ZIF-67 are consistent with those of VSM. The interval 1143–1306 cm^{-1}, is related to the vibration of the imidazole ring. The telescopic vibration of M-ZIF-8@ZIF-67, associated with the peak located at 993–1100 cm^{-1}, is as a result of the C=N bond in ZIF-67, suggesting that ZIF-67 is perfectly conjugated to the surface of M-ZIF-8. The peak generated by the C—N stretching vibration is located at 1420 cm^{-1}, and for the N—H stretching vibration, the assigned peak is located at 2920 cm^{-1}. The peak generated by the stretching vibration of the C—H bond associated with the

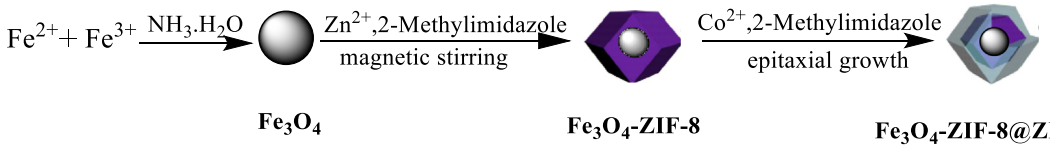

Fig. 1. Diagrammatic sketch of the synthesis of a double-layer metal–organic framework (MOF).

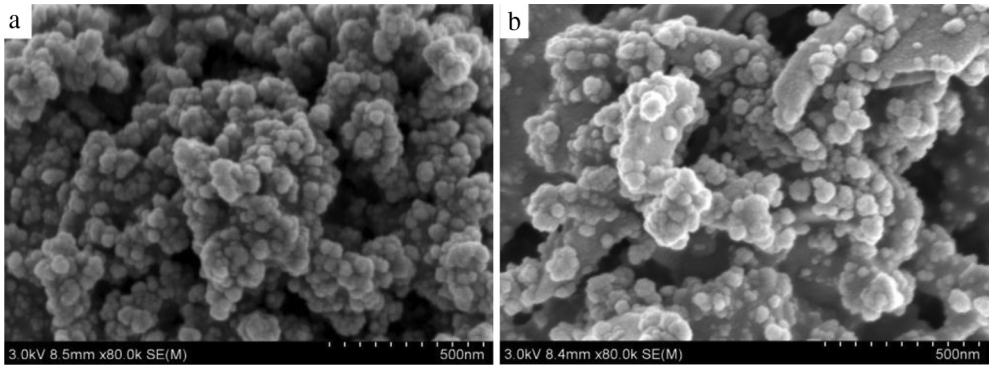

Fig. 2. Scanning electron microscopy micrographs of: (a) Fe_3O_4-ZIF-8 and (b) Fe_3O_4-ZIF-8@ZIF-67.

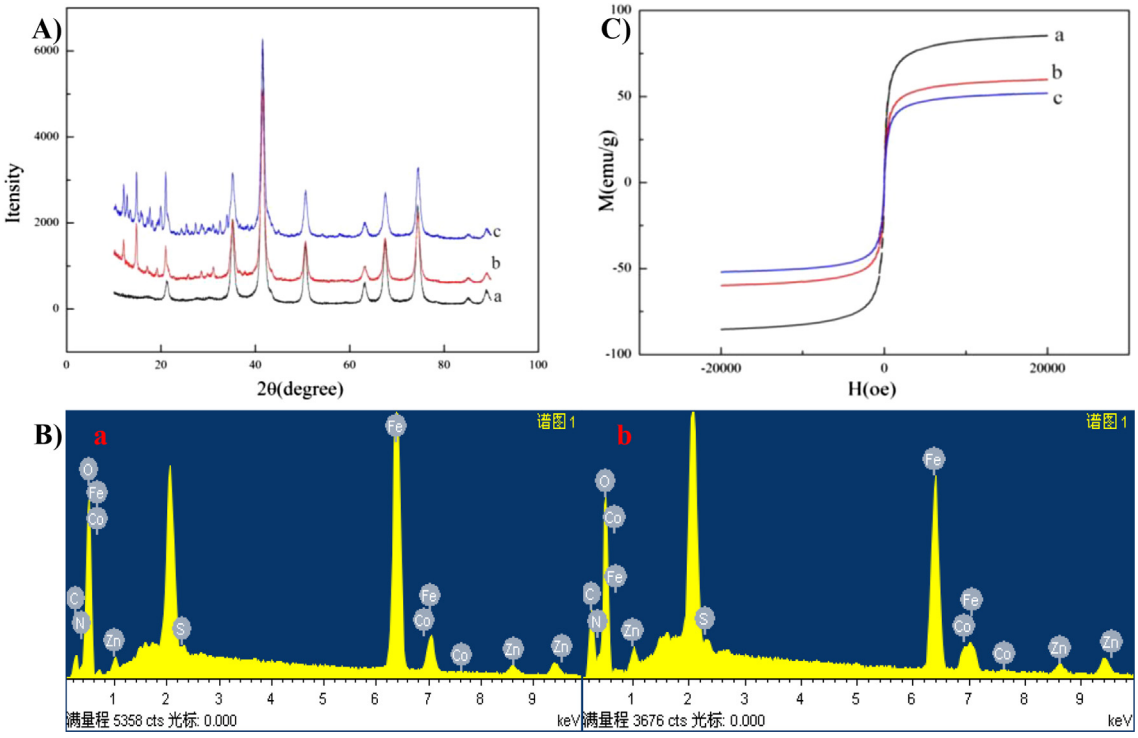

Fig. 3. (A) X-ray diffraction patterns of (a) Fe_3O_4, (b) Fe_3O_4-ZIF-8, and (c) Fe_3O_4-ZIF-8@ZIF-67. (B) Energy-dispersive X-ray spectroscopy image of (a) M-ZIF-8 and (b) M-MOF, (C): magnetic hysteresis loops of (a) Fe_3O_4, ((b) Fe_3O_4-ZIF-8, and (c) Fe_3O_4-ZIF-8@ZIF-67.

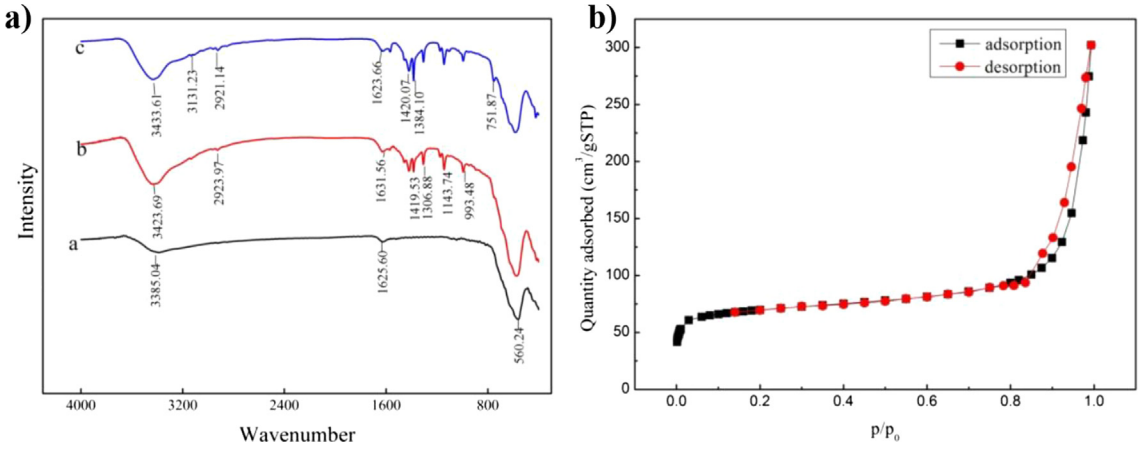

Fig. 4. (a) FT-IR spectra of the synthesized materials, ((b) N_2 sorption-desorption isotherm of M-ZIF-8@ZIF-67.

2-methylimidazolium ring is positioned at 2921–3131 cm^{-1}. The diffraction peak shift of M-ZIF-8 and M-ZIF-8@ ZIF-67 are the same as that of Fe_3O_4, which indicates that the materials are magnetic and that the structure of Fe_3O_4 is retained in the synthesis of the subsequent polymer. The intensities of the XRD patterns demonstrate that the composites possess high crystallinity, consistent with the FT-IR spectra, and furthermore, show that the synthesized ZIF-67 was incorporated into the M-ZIF-8 material without comprising the structural integrity of the M-MOF skeleton.

The textural properties of M-MOF were verified by N_2 adsorption-desorption isotherm measurements [30]. Fig. 4b shows the isotherm of the prepared product. The shape of the N_2 adsorption-desorption isotherm indicates the presence of both micropores and macropores of different sizes in the material. The adsorption curve shows rapid uptake of N_2 in the micropores at low pressures. The isotherm plateaus across a P/P_0 range of 0.1–0.8, indicating adsorption on the surface of the material [31]. The small hysteresis loop is observed as a result of particle packing or by condensation within the interstitial sites of the macroporous structure [32]. The Brunauer-Emmett-Teller (BET) surface area and pore volume of the M-MOF material are 219 m^2/g and 0.07 cm^2/g, respectively. The results show that the surface area of the material was effective for the adsorption of the fipronil and its metabolites [33,34].

Adsorption capacity studies

To test and verify the static adsorption capacity of the double layer M-MOF material for pesticide uptake, measurements were obtained, as shown in Fig. 5a. The adsorption of pesticides increases with the increase of pesticide concentration. However, the adsorption capacity reached equilibrium at 10 mg/L. The adsorption capacities for fipronil desulfiny, fipronil, fipronil sulfide and fipeonil sulfone in the solution supernatant, determined by HPLC-MS/MS at 10 mg/L, were 3.244, 3.955, 5.188 and 5.729 mg/L, respectively. Fig. 5b shows the total ion chromatogram of the fipronil desulfiny, fipronil, fipronil sulfide and fipeonil sulfone. In the absence of optimization of other conditions, M-ZIF-8@ZIF-67 exhibits a high adsorption capacity because of the double-layer structure of the M-ZIF-8@ZIF-67 material having a large surface adsorption capacity and uniform micropores. Adsorption isotherms describe the adsorption relationship between the adsorbent and adsorbate. Static adsorption was tested by the Langmuir and Freundlich models. As shown by the correlation coefficient (R^2) values, the Freundlich model is more suitable for static adsorption of pesticides than the Langmuir model (Table 1). The static adsorption ability of the fipronil desulfiny, fipronil, fipronil sulfide and fipeonil sulfone were in accordance with the Freundlich bimolecular layer adsorption, which indicates that the double-layer M-ZIF-8@ZIF-67 material has been successfully applied to pesticide adsorption.

In order to examine the mechanism of adsorption process, a pseudo-second-order model was established. The pseudo-first-order and intraparticle quadratic fusion models have been studied in other literatures [35], Fig. 5b shows the adsorption kinetics curves (time, *t* vs extraction rate, %) for fipronil desulfiny, fipronil, fipronil sulfide and fipeonil adsorbed by M-ZIF-8@ZIF-67. The adsorption curves reach equilibrium after 45 min of adsorption, with a higher rate of adsorption observed during the first 15 min. The adsorption rate of M-ZIF-8@ZIF-67 is twice faster than that of Ce@ZSM5 [36]. Quasi-second-order kinetic fitting parameters were compared for the adsorption of pesticides (10 mg/L) as a function of time. A demonstrable linear relationship between *t* and *t/Qt* is observed, with the R^2 value approaching 1 (Table 2). The results indicate that the kinetic process of the M-ZIF-8@ZIF-67 adsorption and removal of fipronil desulfiny, fipronil, fipronil sulfide and fipeonil are in accordance with the quasi-second-order kinetic model.

Single-factor experiments to optimize pesticide adsorption

To deduce the optimal extraction parameters, the pH value of the solution, the mass of the M-ZIF-8@ZIF-67 adsorbent, and the ion salt concentration during the adsorption of pesticides were obtained.

Table 1
Fitting parameters of langmuir and freundlich models for M-MOFs adsorbed pesticides.

Model analysis	Fipronil and derivatives	Calibration equation	R^2
Freundlich	Fipronil desulfiny	y = −0.7546x + 0.0232	0.9827
	Fipronil	y = −0.7787x + 0.0292	0.9704
	Fipronil sulfide	y = −0.8008x − 0.675	0.9729
	Fipeonil sulfone	y = −0.824x − 0.4469	0.9628
Langmuir	Fipronil desulfiny	y = −0.6684x + 9.7983	0.1484
	Fipronil	y = −0.7062x + 10.474	0.1272
	Fipronil sulfide	y = −0.6372x + 8.4103	0.125
	Fipeonil sulfone	y = −0.7641x + 9.0046	0.1258

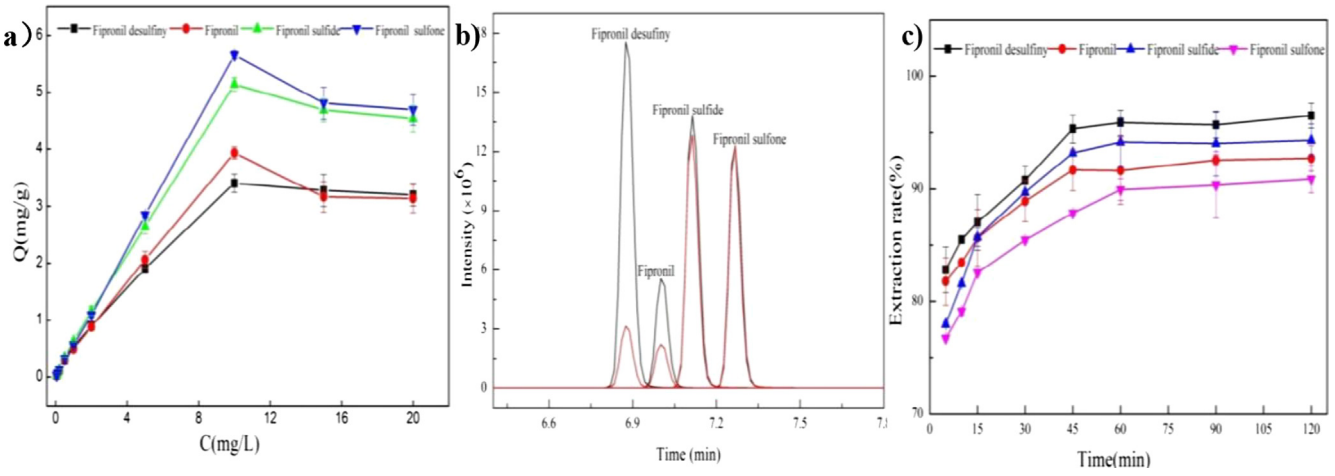

Fig. 5. (a) Adsorption isotherms relating to pesticide uptake on M-M-ZIF-8. (b) The ion chromatograms of the four pesticides. (c) Dynamic adsorption curves of the pesticides.

Table 2
Fitting parameters of the adsorption isotherms of four pesticides on metal–organic framework (MOF) by quasi-second-order equations.

Model analysis	Fipronil and derivatives	Calibration equation	R^2
Pseudo-second-order	Fipronil desulfiny	y = 5.6034x + 1.0956	0.9983
	Fipronil	y = 6.0466x – 0.7766	0.9976
	Fipronil sulfide	y = 4.7527x – 0.2679	0.9981
	Fipeonil sulfone	y = 4.6515x – 1.0427	0.9976

Effect of pH on adsorption capacity of M-MOFs

The pH of the solution not only affects the surface charge-carrying properties of the adsorbent, but also changes the adsorption state of the target. The adsorption mechanism of adsorbents may involve electrostatic interactions, acid-base interactions and π-π interactions [37]. The pH value of the solution is observed to be within the range of 2–10, with the highest adsorption efficiency attained at pH 6 (Fig. 6a). This observation may be attributed to two reasons: first, the pH value of the solution is adjusted by NaOH or HCl. The extraction rate at pH < 6 is higher than that at pH > 6. The Co ion may be incompletely coordinated in the metal framework, and with increasing —OH ion concentration, the binding sites of the pesticides are occupied to a greater extent attributed to the combination of —OH ions and Co ions, which results in a decrease of the extraction rate; second, the electrostatic interactions between M-ZIF-8@ZIF-67 and the pesticide can improve the extraction rate under weakly acidic conditions, leading to a higher extraction rate at pH 6 when compared with pH 7.

Effect of M-MOF content

The influence of adsorbent amount on optimizing the adsorption and removal of pesticides was determined (Fig. 6b). Other experimental variables for pesticide uptake were fixed: pesticide concentration 10 mg/L, pH 6, and a contact time of 45 min. With increasing adsorbent amount, the extraction rate was also observed to increase, with a maximum extraction rate obtained at an adsorbent loading of 15 mg. When further increasing the adsorption content from 15 mg to 40 mg, the extraction rate reached a state of equilibrium. The extraction rates of the four pesticides were all >80%.

Effect of the ionic strength

The effect of the ionic strength on the adsorption and removal of the four pesticides by the M-MOF material was investigated by varying the ion salts-NaAc, KCl, Na_2CO_3. Other experimental variables for pesticide uptake were fixed: pesticide concentration 10 mg/L, pH 6, extraction time 45 min, and M-ZIF-8@ZIF-67 content of 15 mg. The extraction rate is observed to be higher for low ion concentrations when compared with high ion concentrations (Fig. 6c), with pesticides extraction rate of <80%. High salt concentrations will influence the mass transfer rate of the pesticide molecules and affect the electrostatic interactions resulting in a

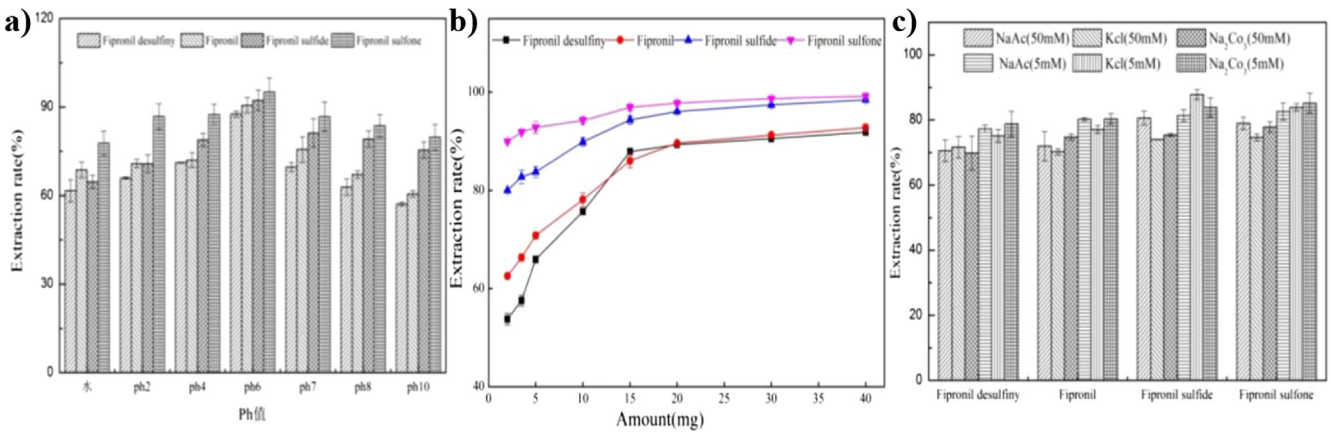

Fig. 6. (a) Effect of: (a) pH, (b) adsorbent amount and (c) ionic strength for the extraction efficiency of pesticides.

Table 3
Pesticide uptake and recovery in the presence of M-MOF as a function of pesticide concentration in environmental water.

Pesticide	Spiked (μg/L)	Tap water			River water			Ground water		
		Found (μg/L)	Recovery (%)	RSD (%)	Found (μg/L)	Recovery (%)	RSD (%)	Found (μg/L)	Recovery (%)	RSD (%)
Fipronil desulfiny	15	0.24	98.3	0.36	0.37	97.5	0.18	0.17	98.8	1.47
	10	0.21	97.8	0.13	0.24	97.5	0.31	0.20	97.9	0.05
	5	0.08	98.3	1.8	0.11	97.6	0.04	0.12	97.5	0.21
Fipronil	15	0.55	96.3	0.36	0.72	95.1	0.15	0.72	95.2	0.08
	10	0.36	96.3	0.92	0.52	94.7	1.15	0.48	95.1	1.01
	5	0.21	95.6	0.5	0.27	94.4	0.21	0.23	95.3	1.21
Fipronil sulfide	15	0.03	99.7	0.01	0.07	99.4	0.07	0.04	99.7	0.03
	10	0.03	99.6	0.16	0.03	99.6	0.02	0.04	99.5	0.16
	5	0.02	99.4	0.24	0.03	99.2	0.33	0.05	98.9	0.16
Fipronil sulfone	15	0.05	99.6	0.05	0.09	99.3	0.07	0.13	99.0	0.08
	10	0.05	99.4	0.09	0.08	99.1	0.46	0.04	99.5	0.04
	5	0.06	98.6	0.25	0.07	98.5	0.12	0.07	98.4	0.04

Table 4
Pesticide uptake and recovery in the presence of M-MOF as a function of pesticide concentartion in cucumber samples.

Pesticide	Spiked (μg/L)	Found (μg/L)	Recovery (%)	RSD (%)
Fipronil desulfiny	200	26.5	86.7	0.70
	100	14.8	85.1	3.83
	50	9.7	87.8	1.78
	20	2.4	87.9	2.68
	5	1.9	86.7	0.78
Fipronil	200	53.8	73.0	1.31
	100	28.7	71.2	2.69
	50	20.2	74.6	2.27
	20	5.3	73.1	2.23
	5	4.3	70.9	1.09
Fipronil sulfide	200	1.1	99.4	0.04
	100	0.9	99.0	0.62
	50	0.44	99.4	0.05
	20	0.17	99.1	0.17
	5	0.2	98.5	0.37
Fipronil sulfone	200	0.85	99.5	0.02
	100	0.61	99.3	0.32
	50	0.37	99.5	0.05
	20	0.16	99.1	0.06
	5	0.26	98.2	0.51

significant decrease of the adsorption rate. The interactions between the spatial structure of M-ZIF-8@ZIF-67 and the pesticide molecules are not influenced by the ion salt concentration [38].

Removal of pesticides from environmental water and cucumber samples

Because MOFs have good adsorption ability in aqueous phase, the spiked pesticide in cucumber homogenization was extracted with water. After that, MOFs mixed with the extraction solution to adsorb the target pesticides. Therefor to verify the efficiency of pesticide uptake more accurately, different concentrations of pesticides (fipronil desulfiny, fipronil, fipronil sulfide, and fipeonil sulfone) were added to the blank sample waters and cucumbers. Pesticide uptake under optimized conditions in the presence of M-ZIF-8@ZIF-67 show that the pesticides were adsorbed and removed by the M-MOF sample at high recovery rates (Tables 3 and 4). Based on the results of the physical structure and chemical adsorption properties of the material, we believe that the material has better adsorption and removal ability for fipronil in water and vegetables, and it is expected to be developed as a solid adsorbent for vegetable quality and safety detection and monitoring.

Comparison of adsorption of fipronil and metabolites with other adsorbents

In this experiment, the adsorption rate, adsorption time, adsorption samples were compared with other adsorbents for adsorption of fipronil and metabolites (Table S2). It is concluded that the adsorbent has a high adsorption rate for the adsorption of fipronil and metabolites, and the experimental operation is time-saving and has great potential for simultaneous application in complex matrices.

Conclusions

In this study, the M-ZIF-8@ZIF-67 were successfully synthesized and used as adsorbent for fipronil desulfiny, fipronil, fipronil sulfide, and fipeonil sulfone. The characterization results suggested that M-ZIF-8@ZIF-67 has double-layer structure and a polyhedron structure with uniform pores, coated on the Fe_3O_4-ZIF-8 surface. The adsorption experiments indicated M-ZIF-8@ZIF-67 has high adsorption ability for fipronil and its metabolites, while more than 95% of the target in ambient water and cucumber samples had been adsorbed and removed. Moreover, the adsorption data well fitted the Freundlich Bimolecular layer adsorption model. A possible mechanism is the bilayer structure of ZIF-8@ZIF-67 composite material exhibits numerous similar pore structures, which enhances the adsorption and removal of organic pollutants. This study showed that M-ZIF-8@ZIF-67 has significant potential for adsorption and removal of fipronil and its metabolites in water and vegetable samples.

Compliance with ethics requirements

All authors have read and approved this version of the paper. We hereby certify that no part of this paper has been published, and it is not under consideration for publication elsewhere. We have carefully checked every aspect of our manuscript in accordance with the author guidelines. We trust that this manuscript is acceptable to meet with your requirement and further review. We hope you will give favorable consideration to this manuscript, and we look forward to receiving comments from the reviewers.

Declaration of Competing Interest

The authors declare no conflict of interest.

Acknowledgements

This work was supported by the National Natural Science Foundation of China (No. 31701695), Agricultural Science and Technology Innovation Program of CAAS, China (CAAS-ZDRW202011) and Scientific Research Project of Hebei Province Education Department (No. QN2018159).

Appendix A. Supplementary material

Supplementary data to this article can be found online at https://doi.org/10.1016/j.jare.2020.03.013.

References

[1] Boulanouar S, Combès A, Mezzache S, Pichon V. Synthesis and application of molecularly imprinted polymers for the selective extraction of organophosphorus pesticides from vegetable oils. J Chromatogr A 2017;1513:59–68. doi: https://doi.org/10.1016/j.chroma.2017.07.067.
[2] Beaudegnies R, Edmunds AJF, Fraser TEM, Hall RG, Hawkes TR, Mitchell G, et al. Herbicidal 4-hydroxyphenylpyruvate dioxygenase inhibitors-A review of the triketone chemistry story from a Syngenta perspective. Bioorganic Med Chem 2009;17:4134–52. doi: https://doi.org/10.1016/j.bmc.2009.03.015.
[3] Ahmed MB, Zhou JL, Ngo HH, Guo W, Thomaidis NS, Xu J. Progress in the biological and chemical treatment technologies for emerging contaminant removal from wastewater: a critical review. J Hazard Mater 2017;323:274–98. doi: https://doi.org/10.1016/j.jhazmat.2016.04.045.
[4] Handford CE, Elliott CT, Campbell K. A review of the global pesticide legislation and the scale of challenge in reaching the global harmonization of food safety standards. Integr Environ Assess Manag 2015;11:525–36. doi: https://doi.org/10.1002/ieam.1635.
[5] Darabdhara G, Boruah PK, Hussain N, Borthakur P, Sharma B, Sengupta P, et al. Magnetic nanoparticles towards efficient adsorption of gram positive and gram negative bacteria: an investigation of adsorption parameters and interaction mechanism. Colloids Surfaces A Physicochem Eng Asp 2017;516:161–70. doi: https://doi.org/10.1016/j.colsurfa.2016.12.003.
[6] Wu ZJ, Jiang BF, Liu WM, Bin Cao F, Wu XR, Li LS. Selective recovery of valuable components from converter steel slag for preparing multidoped FePO 4. Ind Eng Chem Res 2011;50:13778–88. doi: https://doi.org/10.1021/ie202255g.
[7] Kusmiyati, Puspita Adi L, Deni V, Robi IS, Islamica D, Fuadi M. Removal of vertigo blue dyes from Batik textile wastewater by adsorption onto activated carbon and coal bottom ash. AIP Conf Proc 2016:1725. doi: https://doi.org/10.1063/1.4945490.
[8] Choumane FZ, Benguella B. Removal of acetamiprid from aqueous solutions with low-cost sorbents. Desalin Water Treat 2016;57:419–30. doi: https://doi.org/10.1080/19443994.2014.966332.

[9] Dias EM, Petit C. Towards the use of metal-organic frameworks for water reuse: a review of the recent advances in the field of organic pollutants removal and degradation and the next steps in the field. J Mater Chem A 2015;3:22484–506. doi: https://doi.org/10.1039/c5ta05440k.
[10] Hasan Z, Jhung SH. Removal of hazardous organics from water using metal-organic frameworks (MOFs): plausible mechanisms for selective adsorptions. J Hazard Mater 2015;283:329–39. doi: https://doi.org/10.1016/j.jhazmat.2014.09.046.
[11] Liu G, Li L, Xu D, Huang X, Xu X, Zheng S, et al. Metal–organic framework preparation using magnetic graphene oxide–β-cyclodextrin for neonicotinoid pesticide adsorption and removal. Carbohydr Polym 2017;175:584–91. doi: https://doi.org/10.1016/j.carbpol.2017.06.074.
[12] Chin M, Cisneros C, Araiza SM, Vargas KM, Ishihara KM, Tian F. Rhodamine B degradation by nanosized zeolitic imidazolate framework-8 (ZIF-8). RSC Adv 2018;8:26987–97. doi: https://doi.org/10.1039/c8ra03459a.
[13] Fan X, Wang W, Li W, Zhou J, Wang B, Zheng J, et al. Highly porous ZIF-8 nanocrystals prepared by a surfactant mediated method in aqueous solution with enhanced adsorption kinetics. ACS Appl Mater Interfaces 2014;6:14994–9. doi: https://doi.org/10.1021/am5028346.
[14] Tian F, Cerro AM, Mosier AM, Wayment-Steele HK, Shine RS, Park A, et al. Surface and stability characterization of a nanoporous ZIF-8 thin film. J Phys Chem C 2014;118:14449–56. doi: https://doi.org/10.1021/jp5041053.
[15] Wang J, Zhang W, Wei J. Fabrication of poly(β-cyclodextrin)-conjugated magnetic graphene oxide by surface-initiated RAFT polymerization for synergetic adsorption of heavy metal ions and organic pollutants. J Mater Chem A 2019;7:2055–65. doi: https://doi.org/10.1039/c8ta09250h.
[16] Saliba D, Ammar M, Rammal M, Al-Ghoul M, Hmadeh M. Crystal growth of ZIF-8, ZIF-67, and their mixed-metal metabolites. J Am Chem Soc 2018;140:1812–23. doi: https://doi.org/10.1021/jacs.7b11589.
[17] Liu Z-Q, Cheng H, Li N, Ma TY, Su Y-Z. $ZnCo_2O_4$ quantum dots anchored on nitrogen-doped carbon nanotubes as reversible oxygen reduction/evolution electrocatalysts. Adv Mater 2016;28:3777–84. doi: https://doi.org/10.1002/adma.201506197.
[18] Bai S, Jiang W, Li Z, Xiong Y. Surface and interface engineering in photocatalysis. ChemNanoMat 2015;1:223–39. doi: https://doi.org/10.1002/cnma.201500069.
[19] Kuo CH, Tang Y, Chou LY, Sneed BT, Brodsky CN, Zhao Z, et al. Yolk-shell nanocrystal@ZIF-8 nanostructures for gas-phase heterogeneous catalysis with selectivity control. J Am Chem Soc 2012;134:14345–8. doi: https://doi.org/10.1021/ja306869j.
[20] Yang J, Zhang F, Lu H, Hong X, Jiang H, Wu Y, et al. Hollow Zn/Co ZIF particles derived from core-shell ZIF-67@ZIF-8 as selective catalyst for the semi-hydrogenation of acetylene. Angew Chemie - Int Ed 2015;54:10889–93. doi: https://doi.org/10.1002/anie.201504242.
[21] Cho HY, Kim J, Kim SN, Ahn WS. High yield 1-L scale synthesis of ZIF-8 via a sonochemical route. Microporous Mesoporous Mater 2013;169:180–4. doi: https://doi.org/10.1016/j.micromeso.2012.11.012.
[22] Zhang T, Zhang X, Yan X, Kong L, Zhang G, Liu H, et al. Synthesis of Fe_3O_4@ZIF-8 magnetic core-shell microspheres and their potential application in a capillary microreactor. Chem Eng J 2013;228:398–404. doi: https://doi.org/10.1016/j.cej.2013.05.020.
[23] Salunkhe RR, Kamachi Y, Torad NL, Hwang SM, Sun Z, Dou SX, et al. Fabrication of symmetric supercapacitors based on MOF-derived nanoporous carbons. J Mater Chem A 2014;2:19848–54. doi: https://doi.org/10.1039/c4ta04277h.
[24] Zhang T, Du J, Xi P, Xu C. Hybrids of cobalt/iron phosphides derived from bimetal-organic frameworks as highly efficient electrocatalysts for oxygen evolution reaction. ACS Appl Mater Interfaces 2017;9:362–70. doi: https://doi.org/10.1021/acsami.6b12189.
[25] Huang X, Liu Y, Liu G, Li L, Xu X, Zheng S, et al. Preparation of a magnetic multiwalled carbon nanotube@polydopamine/zeolitic imidazolate framework-8 composite for magnetic solid-phase extraction of triazole fungicides from environmental water samples. RSC Adv 2018;8:25351–60. doi: https://doi.org/10.1039/c8ra05064c.
[26] Yang Q, Wang J, Chen X, Yang W, Pei H, Hu N, et al. The simultaneous detection and removal of organophosphorus pesticides by a novel Zr-MOF based smart adsorbent. J Mater Chem A 2018;6:2184–92. doi: https://doi.org/10.1039/c7ta08399h.
[27] Jiang JQ, Yang CX, Yan XP. Zeolitic imidazolate framework-8 for fast adsorption and removal of benzotriazoles from aqueous solution. ACS Appl Mater Interfaces 2013;5:9837–42. doi: https://doi.org/10.1021/am403079n.
[28] Venna SR, Carreon MA. Highly permeable zeolite imidazolate framework-8 membranes for CO_2/CH_4 separation. J Am Chem Soc 2010;132:76–8. doi: https://doi.org/10.1021/ja909263x.
[29] Huang X, Liu G, Xu D, Xu X, Li L, Zheng S, et al. Novel zeolitic imidazolate frameworks based on magnetic multiwalled carbon nanotubes for magnetic solid-phase extraction of organochlorine pesticides from agricultural irrigation water samples. Appl Sci 2018;8:959. doi: https://doi.org/10.3390/app8060959.
[30] Naik B, Hazra S, Prasad VS, Ghosh NN. Synthesis of Ag nanoparticles within the pores of SBA-15: an efficient catalyst for reduction of 4-nitrophenol. Catal Commun 2011;12:1104–8. doi: https://doi.org/10.1016/j.catcom.2011.03.028.
[31] Sahoo B, Sahu SK, Nayak S, Dhara D, Pramanik P. Fabrication of magnetic mesoporous manganese ferrite nanocomposites as efficient catalyst for degradation of dye pollutants. Catal Sci Technol 2012;2:1367–74. doi: https://doi.org/10.1039/c2cy20026k.
[32] Schejn A, Balan L, Falk V, Aranda L, Medjahdi G, Schneider R. Controlling ZIF-8 nano- and microcrystal formation and reactivity through zinc salt variations. CrystEngComm 2014;16:4493–500. doi: https://doi.org/10.1039/c3ce42485e.
[33] Wiebcke M, Cravillon J, Münzer S, Lohmeier SJ, Feldhoff A, Huber K, et al. Rapid room-temperature synthesis and characterization of nanocrystals of a prototypical zeolitic imidazolate framework. Chem Mater 2009;21:1410–2. doi: https://doi.org/10.1021/cm900166h.
[34] Liu Y, Gao Z, Wu R, Wang Z, Chen X, Chan TWD. Magnetic porous carbon derived from a bimetallic metal–organic framework for magnetic solid-phase extraction of organochlorine pesticides from drinking and environmental water samples. J Chromatogr A 2017;1479:55–61. doi: https://doi.org/10.1016/j.chroma.2016.12.014.
[35] Habila MA, ALOthman ZA, Al-Tamrah SA, Ghafar AA, Soylak M. Activated carbon from waste as an efficient adsorbent for malathion for detection and removal purposes. J Ind Eng Chem 2015;32:336–44. doi: https://doi.org/10.1016/j.jiec.2015.09.009.
[36] Rathi A, Basu S, Barman S. Adsorptive removal of fipronil from its aqueous solution by modified zeolite HZSM-5: equilibrium, kinetic and thermodynamic study. J Mol Liq 2019;283:867–78. doi: https://doi.org/10.1016/j.molliq.2019.02.140.
[37] Zhou Q, Wang Y, Xiao J, Fan H. Adsorption and removal of bisphenol A, α-naphthol and β-naphthol from aqueous solution by Fe_3O_4@polyaniline core-shell nanomaterials. Synth Met 2016;212:113–22. doi: https://doi.org/10.1016/j.synthmet.2015.12.008.
[38] Liu G, Li L, Huang X, Zheng S, Xu X, Liu Z, et al. Adsorption and removal of organophosphorus pesticides from environmental water and soil samples by using magnetic multi-walled carbon nanotubes @ organic framework ZIF-8. J Mater Sci 2018;53:10772–83. doi: https://doi.org/10.1007/s10853-018-2352-y.